Two-photon excitation laser scanning microscopy of rabbit nasal septal cartilage following Nd:YAG laser mediated stress relaxation

Charlton C. Kim[*a,b], Vincent Wallace[b], Mariah Coleno[b], Xavier Dao[b],
Bruce Tromberg[b], Brian J.F. Wong[b]

[a]Yale University School of Medicine, New Haven, CT 06510
[b]Beckman Laser Institute and Medical Clinic, Irvine, CA 92612

ABSTRACT

Laser irradiation of hyaline cartilage result in stable shape changes due to temperature dependent stress relaxation. In this study, we determined the structural changes in chondrocytes within rabbit nasal septal cartilage tissue over a 12-day period using a two-photon laser scanning microscope (TPM) following Nd:YAG laser irradiation. During laser irradiation surface temperature, stress relaxation, and diffuse reflectance, were measured dynamically. Each specimen received one or two sequential laser exposures (average irradiation times of 4.5 and 8 seconds). The cartilage reached a peak surface temperature of about 61°C during irradiation. Cartilage denatured in 50% EtOH was used as a positive control. TPM was performed to detect the fluorescence emission from the chondrocytes. Images of chondrocytes were obtained at depths up to 150 microns, immediately following laser exposure, and also following 12 days in culture. Few differences in the pattern or intensity of fluorescence was observed between controls and irradiated specimens imaged immediately following exposure, regardless of the number of laser pulses. However, following twelve days in tissue culture, the irradiated specimens increase, whereas the native tissue diminishes, in intensity and distribution of fluorescence in the cytoplasm. In contrast, the positive control shows only extracellular matrices and empty lacuna, features consistent with cell membrane lysis.

Keywords: Cartilage, microscopy, viability, chondrocyte, two-photon microscopy

1. INTRODUCTION

In head and neck reconstructive surgery, cartilage grafts are carved, sutured, or morselized into new shapes to approximate the geometry of the missing structure. The drawback to these conventional techniques is that excess normal tissue is often discarded and significant donor site morbidity may result. Laser-mediated cartilage reshaping is a new surgical technique which may replace these older operative methods; cartilage is reshaped into complex geometries, via thermal-mediated stress relaxation. The mechanism of action is thought to involve collagen denaturation, alteration of weak van der Waals bonds between proteoglycan molecules, and/or water flux. Mechanical stress relaxation occurs during laser heating; internal stress $\sigma(t)$ (the force exerted by the cartilage resisting external deformation) initially increases, peaks and then rapidly decreases prior to cessation of laser irradiation[1] (**Figure 1**). At the same time, diffuse reflectance $I(t)$ from a visible wavelength probe laser follows a similar temporal pattern to $\sigma(t)$, in that it too peaks and decreases. Previously, we demonstrated that non-contact optical monitoring can be used to assess real-time changes in tissue mechanical properties during laser irradiation and to control the reshaping process[2]. The peak in $I(t)$ observed during laser irradiation indicates the onset of stress relaxation and can be used to modulate laser power or terminate irradiation.

While the biophysical changes accompanying laser reshaping have been characterized [1,3-8], the effect of laser irradiation on chondrocyte viability and metabolism has not been extensively studied. At least three long-term animal studies have been done, that show that overt tissue necrosis and resorption of the graft by the host immune system does not necessarily follow laser-mediated reshaping[9-11]. Histological studies of animal and ex-vivo human issue have demonstrated the absence of classic cytological features associated with cellular necrosis[9,12-15]. In these studies, no measurements were recorded which allowed correlation of these observations with the changes in tissue temperature, optical properties, or internal stress that occur during irradiation.
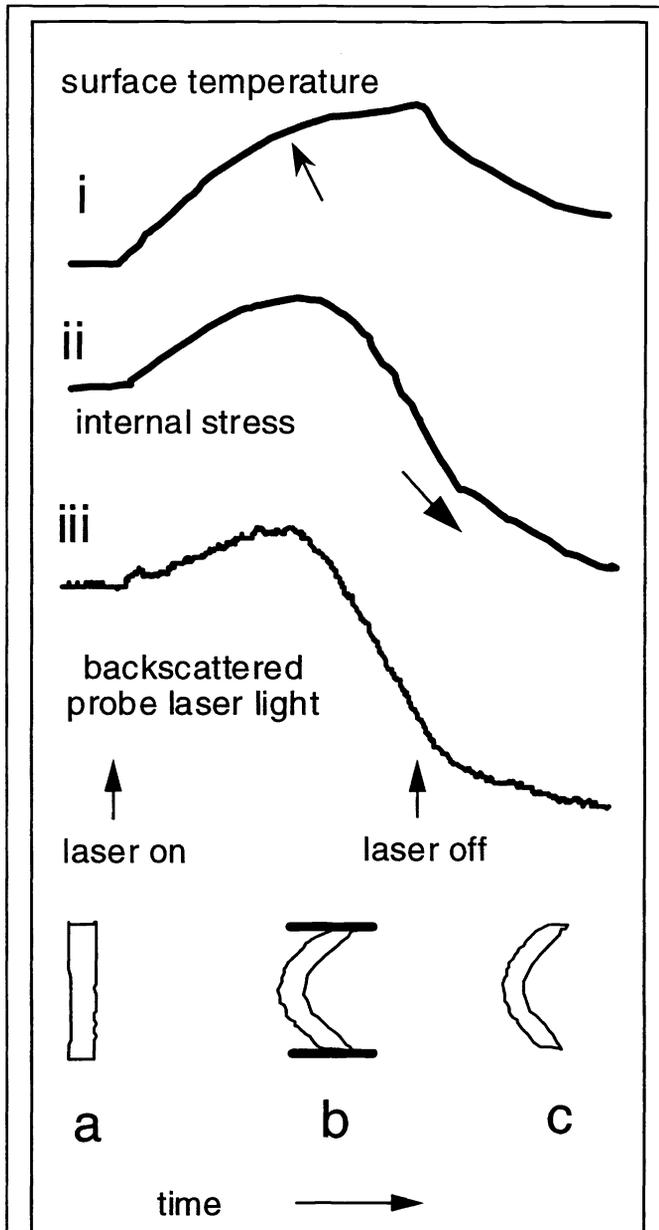
---

[*] correspondence: charlton.kim@yale.edu

Figure 1: Laser-Mediated Cartilage Reshaping. A flat cartilage specimen (a) is held in a reshaping jig (b) during Nd:YAG laser irradiation to create a new shape (c) as surface temperature (i), internal stress (ii), and backscattered HeNe probe laser light (iii) are recorded. When surface temperature reaches about 61°C (arrow) a change in slope of the temperature curve is observed suggesting a change in tissue thermal properties. With the onset of laser irradiation, internal stress initially increases, then at 61°C, internal stress begins to rapidly decrease (large arrow) as reshaping begins (ii). Alterations in measured backscattered probe light (iii) mirror corresponding changes in internal stress.

While conventional light microscopy has been used to examine intact irradiated cartilage specimens, tissue fixation and exogenous dyes are necessary, and as a result serial examination of the same specimen over time is not possible. The objective of this pilot study was to image rabbit nasal septal cartilage after ND:YAG laser (λ=1.32 μm) irradiation using Two-photon microscopy (TPM) in order to assess chondrocyte structural changes and metabolic activity under conditions which simulate those used for reshaping (stress relaxation). Specimens were imaged immediately after laser heating and at 12 days (maintained in tissue culture). The rabbit nasal septum consists primarily of hyaline cartilage. Within the tissue, small chondrocyte aggregates (usually 2-4 cells) are embedded within an extensive matrix containing ground substance and collagen fibers. Chondrocytes are contained within the *lacuna*, a defect in the matrix structure (**Figure 2**). The region of the matrix immediately surrounding the lacuna is often referred to as the *territorial matrix*, and contains a high concentration of acidic, sulphated proteoglycans. The intracellular structure of chondrocyte is similar to most eukaryotic cells. A well-defined nucleus is surrounded by a extensive *rough endoplasmic reticulum* and *Golgi* apparati. In transmission electron micrographs, *nucleoli* and numerous *mitochondria* are identified. In larger chondrocytes, large lipid droplets within the cytoplasm may be a prominent feature[16].

2. MATERIALS AND METHODS

2.1 Tissue harvest

Nasal septal cartilage was obtained from freshly euthanized rabbits (Dark-haired) from Sierra Medical Products (Downey, CA). The specimens were cut into rectangular slabs (15 x 10 mm)[1], and stored in physiological saline at ambient temperature for about 2 hours prior to laser irradiation.

2.2 Biophysical measurements

Diffuse reflectance I(t) from a **HeNe** probe laser (λ= 632.8 nm, 15mW, Melles Griot, Irvine, CA), radiometric surface temperature $S_c(t)$, internal stress $\sigma(t)$ were measured during laser irradiation as previously described (**Figure 3**) [1]. The specimens were irradiated with a **ND:YAG** laser (λ=1.32 μm, 50 Hz Pulse Repetition Rate, NewStar Lasers, Auburn, CA), delivered via a 600 μm core diameter multimode optical fiber. The laser spot size was estimated to be 5.4 mm (power density, 25 W/cm^2). $S_c(t)$ was monitored using a thermopile sensor (Thermalert MI-40, response time of 120 ms (95%), spectral sensitivity of 7.6-18 μm, Raytek, Santa Cruz, CA). The detection system was calibrated as previously described[3].
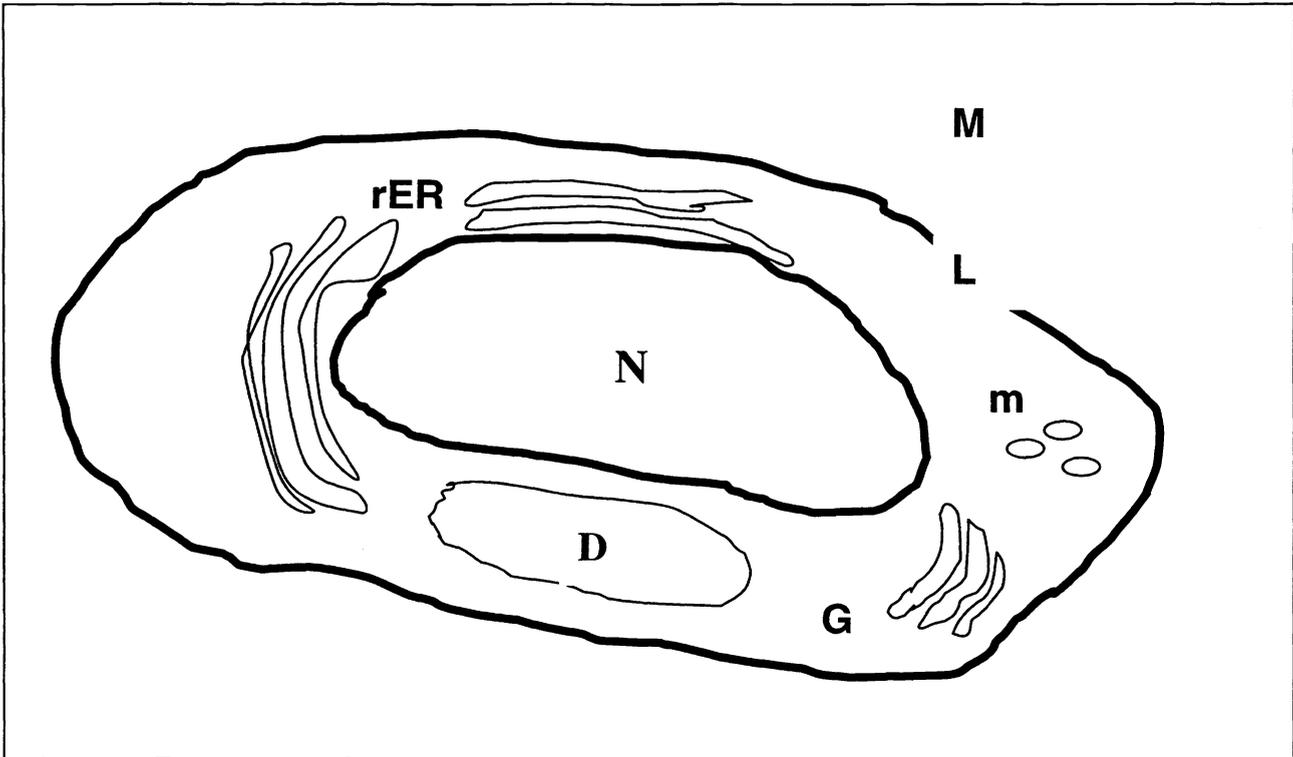
M

rER

L

N

m

D

G

Figure 2: Schematic drawing of a chondrocyte. N-nucleus, M-matrix, L-lacuna, m-mitochondria, rER-rough endoplasmic reticulum, G-Golgi, D-lipid droplet.
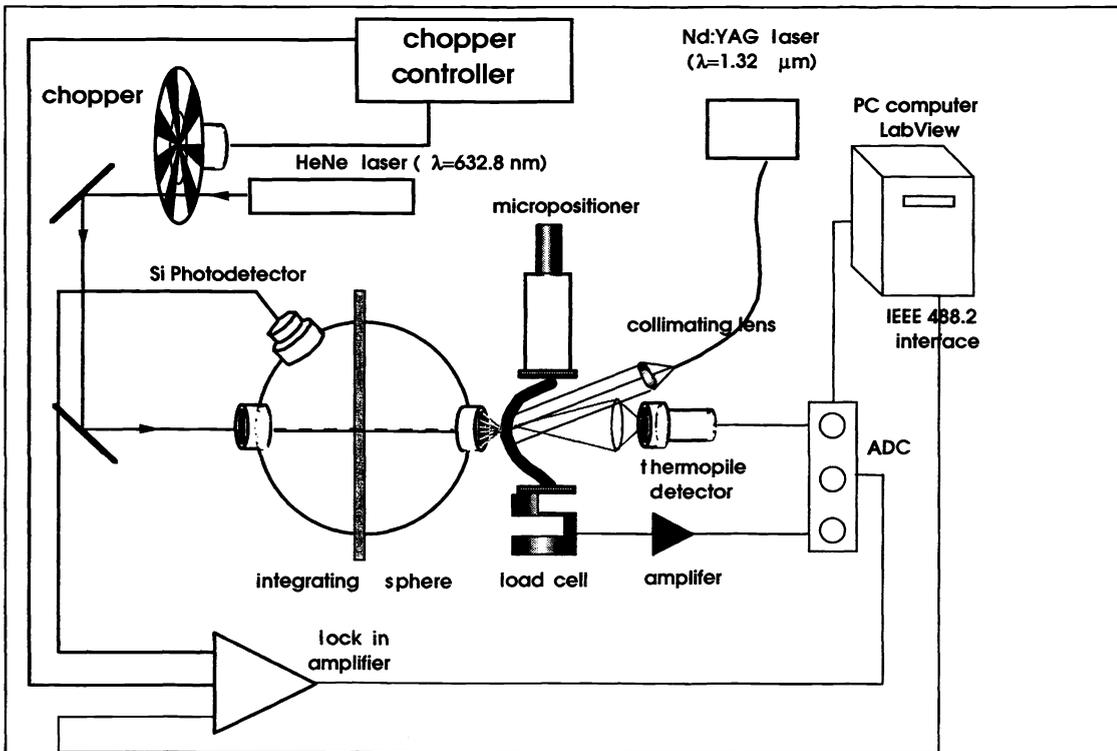
chopper controller

Nd:YAG laser
$(\lambda=1.32 \ \mu m)$

chopper

PC computer LabView

HeNe laser ($\lambda=632.8$ nm)

micropositioner

Si Photodetector

collimating lens

IEEE 488.2 interface

ADC

thermopile detector

integrating sphere | load cell | amplifer

lock in amplifier

Figure 3: Schematic of experimental apparatus.

2.3 Experimental protocol

A schematic of the experimental protocol is illustrated in **Figure 4**. Cartilage specimens were divided into two experimental protocols: **group A)** imaged immediately following tissue harvest or laser irradiation, and **group B)** irradiated and then placed in tissue culture for 12 days prior to imaging. Specimens within each study group were irradiated one or two times with the laser (with a cooling time interval of 5 minutes between each pulse). The duration of each laser exposure was determined by observation of the peak value for $I(t)$ on the read-out of the lock-in amplifier; the laser irradiation was terminated after the peak was identified. Thus, the laser exposure time varied somewhat from sample to sample; however, the average irradiation time for the first, and second exposures were 4.5 and 8 seconds, respectively. Following irradiation, a 6 mm disc was excised from the irradiated region of the specimen, using a biopsy punch. Nicking an edge of the irradiated surface of the disc with a razor blade resulted in a discernible mark that in turn allowed correct specimen orientation. Native cartilage was used as a negative control, and cartilage immersed in 50% EtOH for 20 minutes (and rehydrated in phosphate buffered saline for 10 min.) served as a positive control.
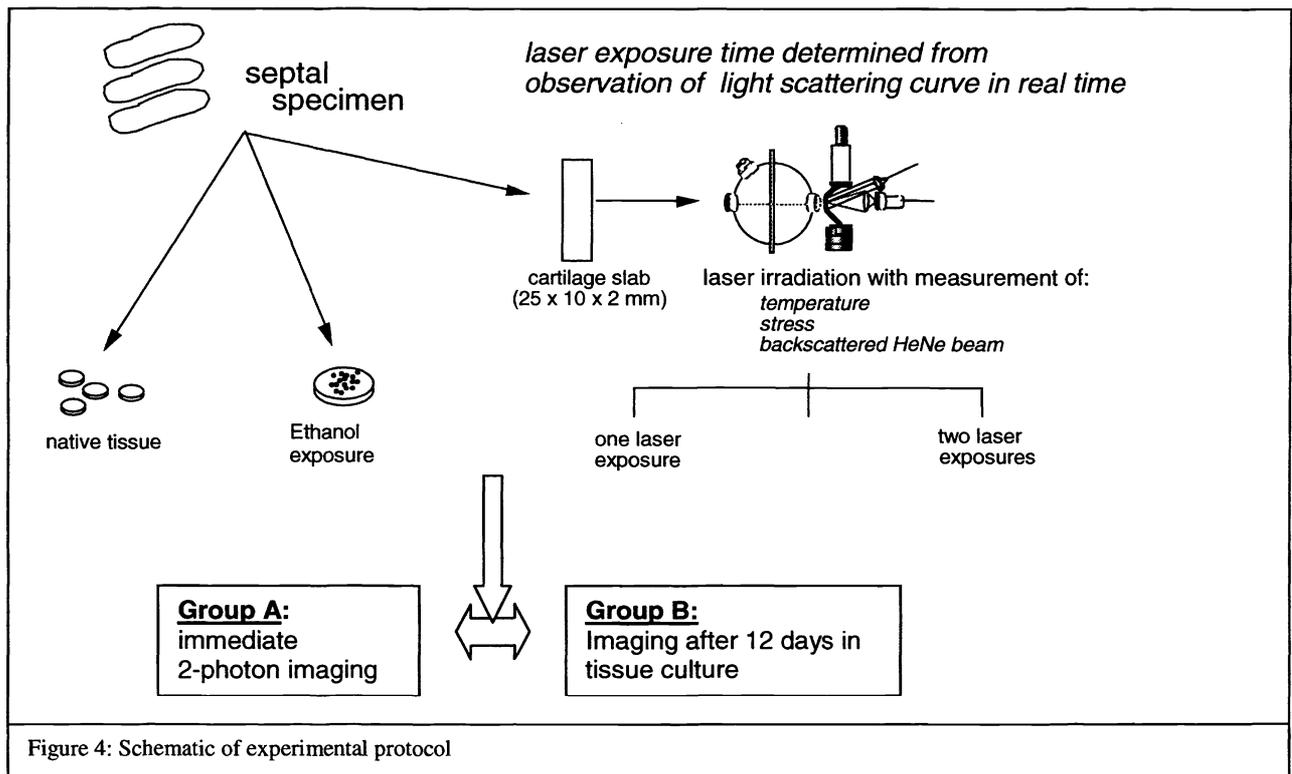

Figure 4: Schematic of experimental protocol

2.4 Tissue culture

The excised discs were placed individually into 24 well culture plates and washed 3 times (15 minutes per wash) with an antibiotic rinse containing gentamycin (200 mg/L) and amphotericin B (22.4 mg/L) in phosphate buffered saline (PBS) (w/o calcium and magnesium). The samples were then incubated (37°C, 5% CO_2) in Dulbelco's Modified Eagle's Medium (DMEM) (Life Technologies/Gibco, Grand Island, NY) containing 10% fetal calf serum (FCS), gentamicin (10 mg/mL), penicillin (100 µg/mL), streptomycin (100µg/mL), and L-glutamine (29.2 g/mL). After 12 days in culture, the specimens were imaged using **TPM**.
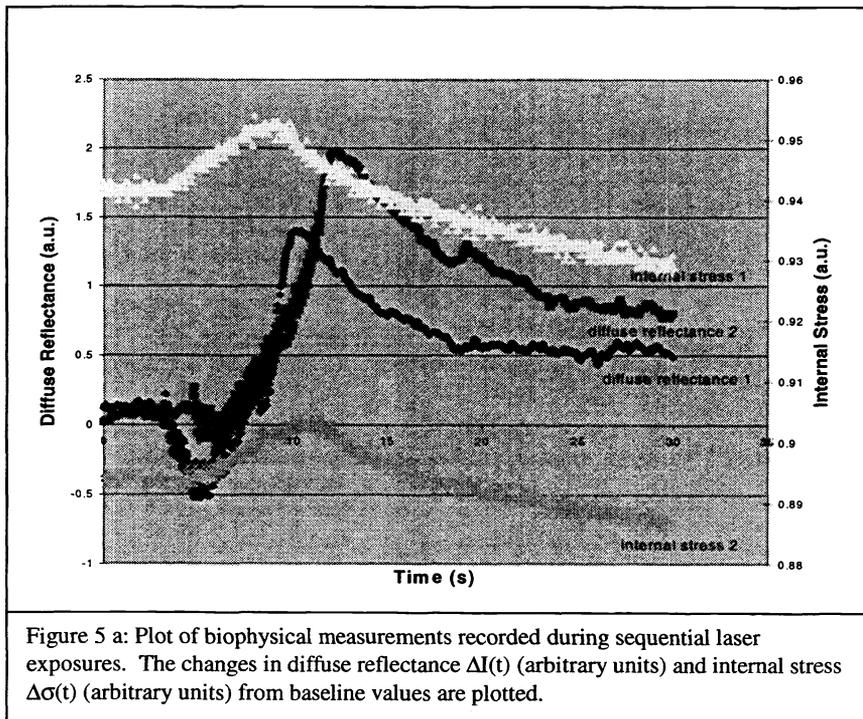
2.5 TPM imaging

The **TPM** device in our laboratory is based on the system constructed by So et al at the Laboratory for Fluorescence Dynamics (LFD) at the University of Illinois at Urbana, Champagne. The system contains a 5W Verdi laser (Coherent, Santa Clara, CA), which acts as a pump for the two photon, pulsed excitation source, Titanium: Sapphire (Ti: Al_2O_3) laser (Mira

900F, Coherent, Santa Clara, CA). Neutral density filters are used to control the average power after the Ti: Sapphire laser, so that the low powers necessary for cell survival could be maintained at the sample, while still maintaining sufficient peak power for two-photon excitation to occur. A mode-locked, 100 femtosecond, 76 MHz pulse train exiting the Ti: Sapphire laser is expanded and collimated using two lenses to overfill the back aperture of the microscope objective. **TPM** was performed using a mode-locked 780nm beam to optimally detect fluorescence from endogenous metabolic components such as **NADH**, **NADPH**, and flavoproteins in the 400-500 nm spectral region. The sample was placed on an inverted Zeiss Axiovert 100 microscope (Zeiss, Thornwood, NY). A small drop of PBS is used to cover the sample, and to minimize refractive mismatches. The Ti: Sapphire beam is scanned across the sample, using a PC-controlled X-Y scanner (Series 603X, Cambridge Technology, Inc., Watertown, MA). A Zeiss 63X, 1.2 N.A. water immersion objective (working distance of 200mm) was used.

The induced fluorescence from the tissue passes through a short pass dichroic beam splitter and is directed to a single photon counting detection system that consists of two PMTs (Hamamatsu Corp., Bridgewater, NJ) which are arranged perpendicularly, and separated by a long-pass dichroic beamsplitter. One PMT is optimized for green light (R7400P), and the other for red light (R7400P-01). This makes it possible to simultaneously detect fluorescence in two different wavelength regions.

TPM images of the specimens were obtained at depths of up to 150 microns (35 μm x 35 μm, lateral resolution). Images were obtained in cartilage specimens irradiated with one or two sequential **ND:YAG** laser exposures, both immediately (within 180 minutes) following irradiation, and after 12 days in tissue culture. Native cartilage (negative control) and cartilage immersed in 50% EtOH for 20 minutes (and rehydrated in phosphate buffered saline for 10 min.) (positive control) were imaged identically.

3. RESULTS

Figure 5 a: Plot of biophysical measurements recorded during sequential laser exposures. The changes in diffuse reflectance $\Delta I(t)$ (arbitrary units) and internal stress $\Delta \sigma(t)$ (arbitrary units) from baseline values are plotted.

An example of the biophysical measurements recorded during photothermal heating is illustrated in **Figure 5**. The changes in diffuse reflectance $\Delta I(t)$ (a.u.) and internal stress $\Delta \sigma(t)$ (a.u.) from baseline values during sequential laser exposures are illustrated in **Figure 5 a**. For clarity, $S_c(t)$ (a.u.) is plotted independently (**Figure 5 b**). Peak surface temperatures of 60 and 61°C (ambient temperature of 25°C) were recorded during the first, and second laser pulses corresponding exposure times of 6.3 and 6.6 sec. The time intervals from onset of laser irradiation and the identification of a peak in $\Delta I(t)$ and $\Delta \sigma(t)$ increased with each successive irradiation as previously observed[2]. Because laser irradiation was terminated when the peak in I(t) was observed on the lock-in amplifier signal monitor, laser pulse durations were longer than the elapsed time at w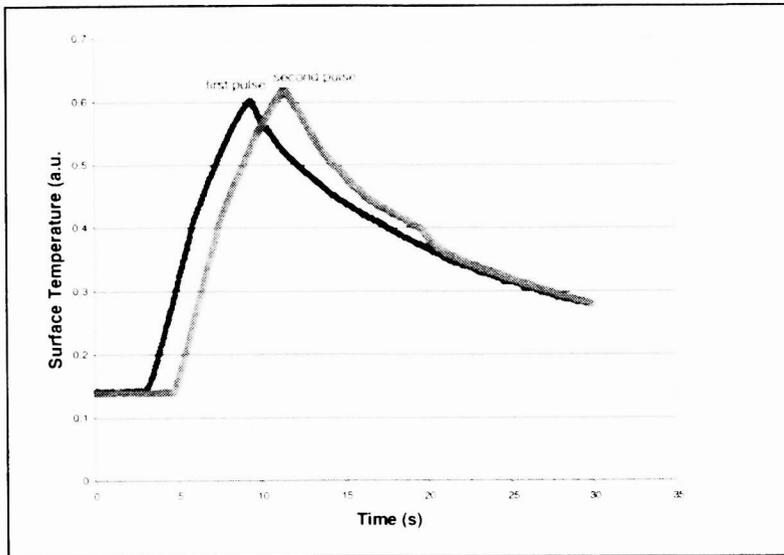hich the peaks in $\Delta I(t)$ and $\Delta \sigma(t)$ were observed. The peak for $\Delta I(t)$ follows the peak for $\sigma(t)$ by about 1 second during both first and second laser exposures.

Representative **TPM** images of chondrocytes within laser irradiated cartilage grafts are illustrated in **Figures 6-7**. I(t), $S_c(t)$, and $\sigma(t)$ were recorded during the irradiation of each specimen with results similar to those illustrated in **Figure 5**.

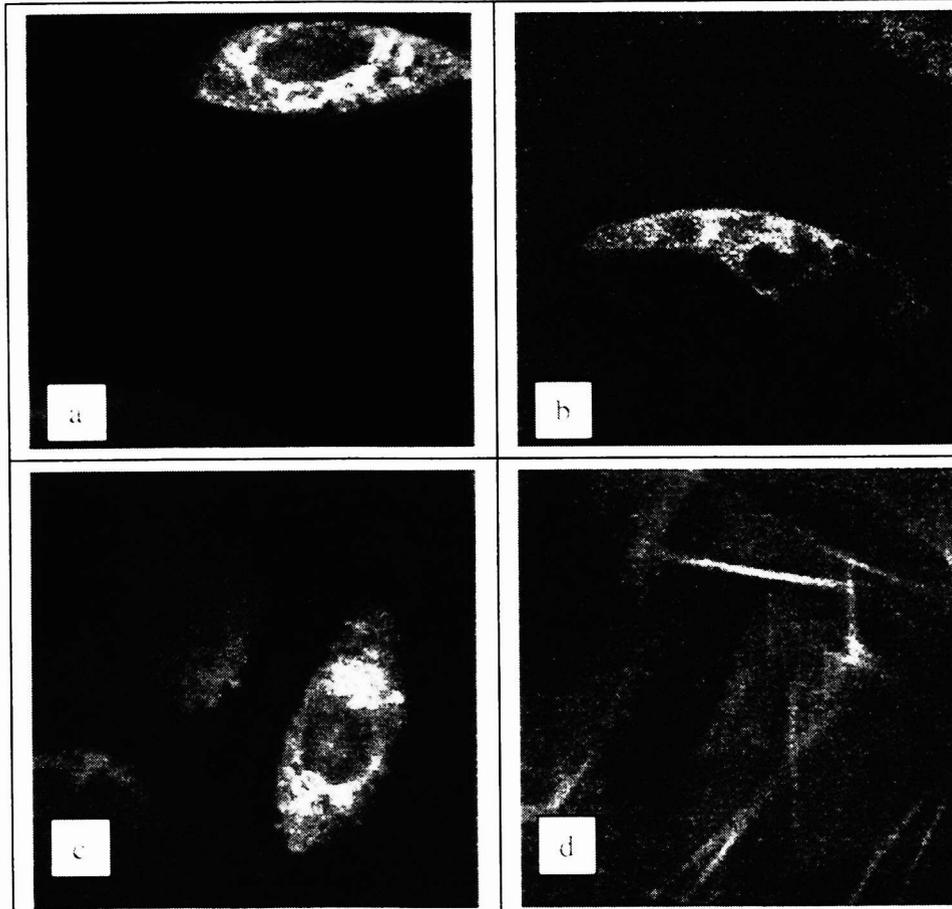Figure 5 b: Plot of surface temperature $S_c(t)$ (arbitrary units) recorded during sequential laser exposures.

In **Figure 6, TPM** images of chondrocytes immediately after laser irradiation (**group A**) are illustrated. The montage is a composite of chondrocytes in cartilage specimens after (**a**) one or (**b**) two laser exposures, (**c**) in non-irradiated native tissue (negative control), and (**d**) of ethanol-denatured cartilage (positive control).

Figure 7 consists of images of laser-irradiated chondrocytes after being maintained in tissue culture for 12 days (**group B**): (**a**) 1 laser exposure, (**b**) two laser exposures, and (**c**) native tissue.

The nucleus can clearly be distinguished from the cytoplasm, and the cell membrane is easily discernible. Large oval regions with low-signal intensity are identified in many cells (**Figure 6 a-c, Figure 7 a-b**), and are likely the nuclei, though it also is possible that they may be large lipid droplets, which are common in large chondrocytes[16]. It is clear that the autofluorescence is concentrated almost exclusively in the cytoplasm, as opposed to the presumed nuclear area. The high fluorescent signal (e.g. **Figure 6 a**) is likely due to the presence of mitochondria, which are rich with **NADH** and **NADPH**. Areas of relatively weak signal (e.g. **Figure 7 a**) may be regions where organelles such as the endoplasmic reticuli and Golgi apparatus are concentrated.

The cell membrane of the chondrocyte does not autofluoresce and hence forms a low-signal intensity rim around the chondrocyte. The matrix immediately adjacent to the cell membrane often does not fluoresce as intensely as matrix further from the cell, and may delineate the *territorial matrix*. (**see Figure 7 b**). The territorial matrix is known to have a high concentration of proteoglycans, and the concentration of collagen in this region may be lower, resulting in less fluorescence than other, more collagen-rich regions of the matrix.

Figure 6: TPM images of porcine chondrocytes immediately after irradiation (Group A). Chondrocytes that underwent one exposure (a), two exposures (b), a non-irradiated, negative control (c), and an ethanol-exposed, positive control (d) are shown.
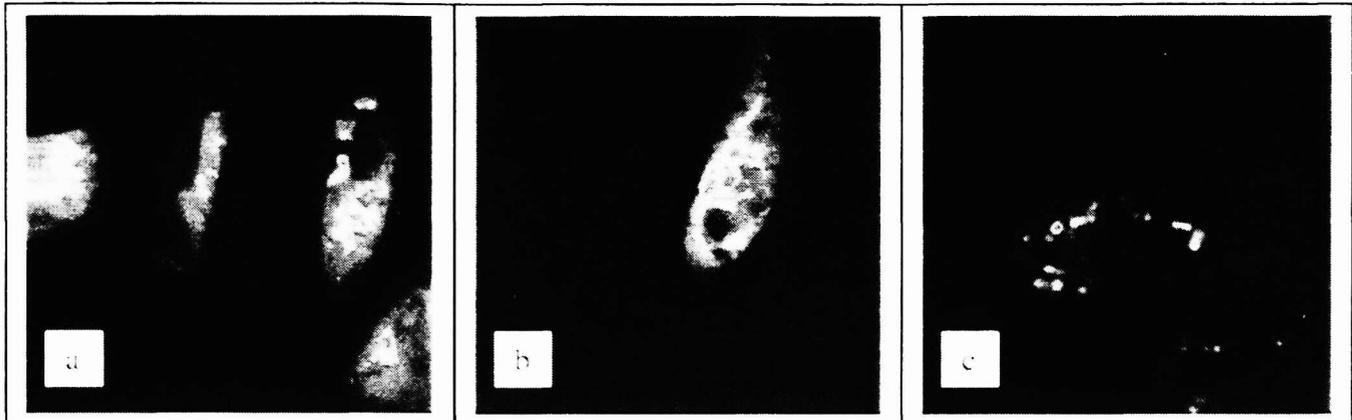
Figure 7: TPM images of chondrocytes following laser irradiation, and 12 days in tissue culture (Group B). Images of cells following 1 exposure (a), 2 exposures (b), and of a non-irradiated, negative control (c), are depicted.

4. DISCUSSION

In reconstructive procedures within the head and neck, autogenous cartilage grafts harvested from heterotopic sites are used to rebuild the damaged framework of facial and airway structures. Often, the graft must be carved, sutured, or morselized in order to recreate the shape of the missing structure. The drawback to these techniques is that excess normal tissue is often discarded, and significant donor site morbidity may result. As a cartilage-sparing alternative, laser irradiation can be used to reshape cartilage grafts into complex shapes, via thermal-mediated stress relaxation. Biochemical assays measuring proteoglycan synthesis have demonstrated that in porcine tissue, PTG synthesis does not decrease markedly after one or two laser exposures, where the pulse duration was determined using optical feedback signals[2]; however PTG synthesis does drop significantly after a third laser exposure. Some studies have suggested that some degree of photothermal heating may actually *stimulate* chondrogenesis[17,18].

In this pilot study, chondrocytes were imaged with **TPM** following **Nd:YAG** laser irradiation using parameters that result in stress relaxation, in order to determine whether significant structural and metabolic injury occurs within the cell, following laser-mediated reshaping. Though studies examining tissue viability following laser irradiation have been performed, most of these only compare tissue response (as determined using histologic, biochemical, or molecular assays) with laser fluence and pulse duration[9-11]. Our study differs from these investigations in that we monitored the thermal, optical, and mechanical properties of cartilage during laser irradiation, and hence were able to correlate the **TPM** images with changes in these biophysical properties. We used the onset of accelerated stress relaxation (representing a change in matrix structure) to terminate laser irradiation in each case.

Functional images were constructed from the excitation of endogenous fluorophores, providing a means to study chondrocyte metabolism. Prior studies have demonstrated that cellular emissions result primarily from the excitation of cellular **NADPH** and **NADH** (concentrated within the mitochondria), which provide an indirect measure of cellular respiration and metabolism[19]. In addition, flavoproteins located in the cytoplasm function as fluorophores, and within the tissue matrix, collagen fibers readily fluoresce as well.

Few differences between the images of the laser-irradiated specimens *(a-b)* and control *(c)* can be observed in **Figure 6**; furthermore, the number of exposures *(one or two)* did not alter the pattern of autofluorescence in specimens imaged right after laser exposure. However, after 12 days in tissue culture (**Figure 7**), the controls (native tissue) exhibit reduced fluorescence, while the intensity and distribution of fluorescence increases in irradiated specimens. As it was shown that the metabolic rate of human stromal keratocytes in the cornea increases after surgical wounding[20], we postulate that this increase may be due to chondrocyte reparative processes and wound healing. Alternatively, the increased autofluorescence may indicate the lysis of metabolite-rich organelles such as mitochondria, which would result in increased cytoplasmic concentrations of NADH and NADPH. The decreased intensity of fluorescence in the native specimen over time in culture may be indicative of slowed metabolism occurring in tissue culture.

After 12 days in culture (**Figure 7**), there is little difference in fluorescence between cartilage exposed to (**a**) one or (**b**) two laser pulses. The control (**Figure 7 c**) shows greatly diminished fluorescence, relative to the irradiated specimens after 12 days (**Figure 7 a, b**), as well as the native tissue that was imaged immediately (**Figure 6 c**).

In contrast to the irradiated and native specimens shown in **Figures 6 a-c** and **7 a-c**, the ethanol-immersed positive control (**Figure 6 d**) shows only extracellular matrices and empty lacuna consistent with cell membrane lysis.

The morphologic and functional observations are at variance with previous findings where chondrocyte proteoglycan (PTG) synthesis following laser irradiation[2] (using a similar experimental protocol as this study) was measured. No "dose response" relationship between chondrocyte structure (**TPM** images) and laser dosimetry was observed. This may be in part due to the selective nature of microscopy in that only a limited number of cells are observed; we focused primarily on imaging cells with intact cellular architecture. Functional/ biochemical assay techniques (such as pulse-chase radiolabelling) measure the bulk response of a tissue to exogenous agents or changes in the physical environment (in this case, photothermal heating). Selective visualization of cells within the laser irradiated matrix may in part account for these observations. However, it is important to note that at least some cells in laser irradiated specimens did not look different from their respective controls.

5. CONCLUSION

Tissue viability can be evaluated using methods that characterize structural and functional aspects of cellular function. **TPM** is a unique method that allows for in vitro imaging to depths of several hundred microns where structural detail is provided based on concentration of fluorophores, principally molecules involved in respiratory transport. This preliminary investigation examined the changes in tissue autofluorescence following photothermal heating. In the sample of chondrocytes examined in this study, no differences in the pattern or intensity of fluorescence was observed between controls and irradiated specimens imaged immediately following exposure, regardless of the number of laser pulses. However, following twelve days in tissue culture, the irradiated specimens increase in fluorescence, whereas the native tissue diminishes in fluorescence. While these results are at variance with functional assays that demonstrate a dose response relationship, it is important to note that at least some chondrocytes are still intact with normal fluorescence patterns, despite repeated photothermal heating. Future work includes a thorough survey of irradiated tissue with TPM and the acquisition of fluorescence spectral information. This will allow identification of physiological changes within cells by looking at spectral alterations of endogenous fluorophores.

ACKNOWLEDGMENTS

REFERENCES

1. B.J.F. Wong, T.E. Milner, H.K. Kim, J.S. Nelson, E.N. Sobol, "Stress relaxation of porcine septal cartilage during ND:YAG laser irradiation," *Journal of Biomedical Optics* **3** (No. 4), 409-414, 1998.
2. B.J.F. Wong, T.E. Milner, H.K. Kim, K. Chao, C. Sun, E.N. Sobol, J.S. Nelson, "Proteoglycan synthesis in porcine nasal cartilage grafts following ND:YAG," *Photochemistry and Photobiology* **in press**, 2000.
3. B.J.F. Wong, T.E. Milner, B. Anvari, "Measurement of radiometric surface temperature and integrated back-scattered light intensity during feedback-controlled laser-assisted cartilage reshaping," *Lasers in Medical Science* **13**, 66-72, 1998.
4. V. Bagratashvili, E.N. Sobol, A. Sviridov, V.K. Popov, A. Omel'chenko, S.M. Howdle, "Thermal and diffusion processes in laser-induced stress relaxation and reshaping of cartilage," *J. Biomechanics* **30**, 813-817, 1997.
5. B.J.F. Wong, T.E. Milner, H.K. Kim, et al., "Critical temperature transitions in laser-mediated cartilage reshaping," *Proceedings SPIE* **3245**, 161-172, 1998.
6. E.N. Sobol, *Phase transformations and ablation in laser-treated solids*, John Wiley, New York, 316-322, 1995.

7. E.N. Sobol, A. Sviridov, V.V. Bagratashvili, et al., "Stress relaxation and cartilage shaping under laser radiation," *Proceedings SPIE* **2681**, 358-363, 1996.
8. E.N. Sobol, M. Kitai, N.S. Jones, A. Sviridov, T.E. Milner, B.J.F. Wong, " Theoretical modeling of heating and structure alterations in cartilage under laser radiation with regard of water evaporation and diffusion dominance," *Proceedings SPIE* **3254,** 54-63, 1998.
9. Z. Wang, M.M. Pankratov, D.F. Perrault, S.M. Shapshay, "Endoscopic laser-assisted reshaping of collapsed tracheal cartilage: a laboratory study," *Annals of Otology, Rhinology, and Laryngology* **105**, 176-181, 1996.
10. Z. Wang, M.M. Pankratov, D.F. Perrault, S.M. Shapshay, "Laser-assisted cartilage reshaping: in vitro and in vivo animal studies," *Proceedings SPIE* **2395**, 296-302, 1995.
11. A. Sviridov, E.N. Sobol, V.V. Bagratashvili, et al., "In vivo study and histological examination of laser reshaping of cartilage," *Proceedings SPIE* **3590**, 222-228, 1999.
12. A. Sviridov, E.N. Sobol, N.S. Jones, J. Lowe, "Effect of Holmium laser radiation on stress, temperature, and structure alterations in cartilage," *Lasers in Medical Science* **13**, 73-77, 1998.
13. Y.M. Ovchinnikov, G.N. Nikiforova, V.M. Svistushkin, et al., "Arbitrary modification of cartilage shape under laser radiation," *Russian Annals Otorhinolaryngology* **3**, 5-10, 1995.
14. E. Helidonis, M. Volitakis, I. Naumidi, G. Veelgrakis, J. Bizakis, P. Christodoulou, "The histology of laser thermo-chondro-plasty," *American Journal of Otolaryngology* **15**, 423-428, 1994.
15. Y.M. Ovchinnikov, V.P. Gamov, A.B. Shekhter, et al., "Use of medical lasers for arbitrary modification of cartilage shape in ENT and plastic surgery," *Russian Annals Otorhinolaryngology* **3**, 21-22, 1996.
16. H.G. Burkitt, B. Young, J.W. Heath, P.J. Deakin, *Wheater's Functional Histology (3rd Ed.)*, ch. 10, Churchill Livingstone, New York, 1993.
17. R.J. Schultz, S. Krishnamurthy, W. Thelmo, J.E. Rodriguez, G. Harvey, "Effects of varying intensities of laser energy on articular cartilage: a preliminary study," *Lasers in Surgery and Medicine* **5**, 577-588, 1985.
18. K.B. Trauner, N.S. Nishioka, T. Flotte, D. Patel, "Acute and chronic response of articular cartilage to Holmium:YAG laser irradiation," *Clinical Orthopaedics and Related Research* **310**, 52-57, 1995.
19. B. Chance, B. Thorell, "Localization and kinetics of reduced pyridine nucleotide in living cells by microfluorometry," *J. Biol. Chem.* **234**, 3044-3050, 1959.
20. B.R. Masters, M.V. Riley, J. Fischbarg, B. Chance, "Pyridine nucleotides of rabbit cornea with histotoxic anoxia," *Exp. Eye Res.* **36**, 1-9, 1983.